

# Computer generation of dense polydisperse sphere packings

Anuraag R. Kansal

*Department of Chemical Engineering, Princeton University, Princeton, New Jersey 08544*

Salvatore Torquato<sup>a)</sup>

*Department of Chemistry and Princeton Materials Institute, Princeton University, Princeton, New Jersey 08544*

Frank H. Stillinger

*Department of Chemistry, Princeton University, Princeton, New Jersey 08544*

(Received 10 June 2002; accepted 9 August 2002)

We present an extension of the Lubachevsky and Stillinger [J. Stat. Phys. **60**, 561 (1990)] packing algorithm to generate packings of polydisperse spheres. The original Lubachevsky–Stillinger algorithm is a nonequilibrium protocol that allows a set of monodisperse spheres to grow slowly over time eventually reaching an asymptotic maximum packing fraction. We use this protocol to pack polydisperse spheres in three dimensions by making the growth rate of a sphere proportional to its initial diameter. This allows us to specify a size distribution of spheres, which is then preserved throughout the growth process (except the mean diameter increases). We use this method to study the packing of bidisperse sphere systems in detail. The packing fractions of the configurations generated with our method are consistent with both previously generated experimental and simulated packings over a large range of volume ratios. Our modified Lubachevsky–Stillinger protocol, however, extends the range of sphere volume ratios well beyond that which has been previously considered using simulation. In doing so, it allows both small volume ratios and large volume ratios to be studied within a single framework. We also show that the modified Lubachevsky–Stillinger algorithm is appreciably more efficient than a recursive packing method.

© 2002 American Institute of Physics. [DOI: 10.1063/1.1511510]

## I. INTRODUCTION

The hard-sphere model is one of the simplest representations of condensed matter systems. Examples of systems that are well described by dense packings of hard-spheres include colloids, amorphous metals, and simple liquids. In many experimental circumstances, however, the component spheres are not uniform in size but rather display some distribution of sizes. While there are several algorithms for generating dense packings of monodisperse spheres,<sup>1–4</sup> comparatively few are effective for polydisperse spheres (see, e.g., Ref. 5 and references therein). In addition, previous efforts have focused on relatively narrow distributions of sphere radii. As shown by Schaertl and Sillescu,<sup>6</sup> increasing polydispersity increases the maximum packing fraction,  $\phi$ , of an amorphous hard sphere system. Accordingly, a method that allows for the investigation of hard sphere packings over a wide range of polydispersity and packing fraction would be valuable.

We present a modification of the concurrent algorithm of Lubachevsky and Stillinger<sup>1</sup> to treat polydisperse systems. The Lubachevsky–Stillinger (L–S) algorithm is essentially a nonequilibrium molecular dynamics simulation in which the spheres grow over time. Once the initial conditions are fixed, the system evolves deterministically. Thus, any randomness in a packing generated with the L–S algorithm is derived

from the initial conditions. This algorithm has a single parameter which represents the sphere growth rate relative to the mean sphere speed. As the spheres grow larger, the collision frequency increases and a maximum packing fraction is asymptotically approached. In monodisperse systems, it has been shown that this maximum packing fraction is dependent on the growth rate of the spheres.<sup>1,7</sup> Roughly speaking, by choosing a high growth rate, the structure of the initial configuration is preserved to some extent leading to a more random final configuration. A slower growth rate allows the spheres more time to equilibrate and so yields more dense, but somewhat more ordered, final systems. If the L–S algorithm is run with a high compression rate, however, the packing fraction of the resulting configurations reaches a plateau at  $\phi_m \sim 0.645$ . Note that if the initial configuration is ordered (e.g., the spheres are placed at the sites of the fcc lattice), the final structures are very likely to remain crystalline, independent of the kinetic parameter chosen. The L–S algorithm also has the attractive property of generating strictly jammed packings for monodisperse sphere systems.<sup>8,9</sup> While the same claim has not been shown to hold for polydisperse systems using the extended method, the use of the same termination condition (a divergence in the rate of collisions) offers some promise that this claim will hold.

Using the extended L–S algorithm, we study the interesting case of a binary mixture of hard spheres of different sizes. It has been shown that such mixtures can have a rich variety of equilibrium phase behaviors.<sup>10–13</sup> An example of

<sup>a)</sup>Author to whom correspondence should be addressed. Electronic mail: torquato@electron.princeton.edu

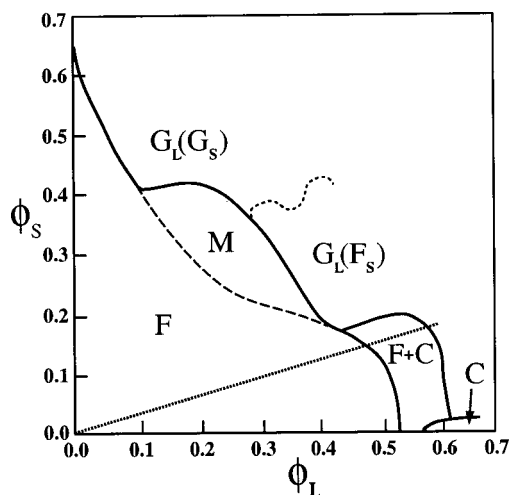


FIG. 1. A schematic of the phase diagram of a binary sphere mixture in which the large spheres have a volume 800 times that of the small spheres. Figure is adapted from Imhof and Dhont (Ref. 12). Solid curves denote phase boundaries. “F” indicates a fluid, “G” a glassy phase, and “C” a crystal phase. Where each size of sphere has different phase behavior, subscripts indicate the size of sphere present in each phase. The “M” indicates a region in which the fluid phase is metastable. The dotted line (emanating from the origin) indicates systems in which the large spheres occupy three times the volume of the small spheres, which is the case in all of the results presented in this work.

the equilibrium phase diagram for a particular binary mixture is shown in Fig. 1. This figure gives the phase diagram for a fixed ratio of sphere volumes. Because we fix the relative volume fraction of large and small spheres, our work represents a cut through this plane (indicated by the dotted line in the figure emanating from the origin). In analogy to the generation of dense packings for monodisperse spheres, it is possible to create amorphous packings of bidisperse spheres at higher packing fractions than the limit of the fluid phase in the equilibrium system. Note that compared to the monodisperse case, hard-sphere systems with some polydispersity tend to remain amorphous over a more broad range of packing fractions. This is evidenced by the large portion of the phase diagram in which fluid or glassy phases are present.

In this paper, we study the maximum packing fraction obtainable for three-dimensional amorphous binary packings using the L–S algorithm as a function of the volume ratio between the two types of spheres. We also present an analytical formula for the packing fraction obtained using a simple recursive method of combining separate packings of large and small spheres. The following section outlines the changes made to the original L–S algorithm to allow polydisperse sphere systems to be generated. Section III details a recursive method of generating dense binary packings by combining two monodisperse packings. Section IV discusses the results of the L–S packing algorithm applied to binary sphere systems. This is followed by some brief concluding remarks in Sec. V.

## II. DESCRIPTION OF THE ALGORITHM

Our adaptation of the L–S algorithm (like the original algorithm) begins with a dilute system of spheres or points. In our adaptation, the initial configuration has a distribution

of sphere volumes. The initial size distribution has the same shape as the desired final distribution, but the radii are decreased by a constant factor. So, for example, to generate a high-density packing with a uniform distribution of sphere volumes such that the largest spheres in the system are twice the volume of the smallest spheres, the algorithm might be initialized with a set of spheres whose volumes are uniformly distributed between 0.5 and 1 (assuming these volumes give a small overall packing fraction). By beginning with a low overall packing fraction ( $\phi \sim 0.35$ ), we are able to use the RSA algorithm<sup>14</sup> to generate an initial packing, which should ensure that our starting configuration is quite random.

The principle modification we perform on the original algorithm is in the treatment of the growth rate. In order to maintain the proper sphere volume distribution, we allow each sphere to grow at its own rate. Like the original algorithm, this approach requires a single parameter,  $\delta$ , to control the rate of growth of the spheres relative to the mean sphere speed. The growth rate of an individual sphere,  $\delta_i$ , is fixed as

$$\delta_i = \delta \sigma_{i,0}, \quad (1)$$

where  $\sigma_{i,0}$  is the initial diameter of the sphere  $i$ . This ensures that the relative distribution of sphere volumes around the mean is constant over time, but the mean sphere volume increases uniformly with time.

Careful attention must be given to the treatment of collisions between spheres in this algorithm. One simple concern regards collisions between spheres of different sizes. The postcollision velocities of spheres will depend on their initial velocities and their masses. We have chosen to give each sphere the same mass in our simulations, effectively assigning a lower internal density to large spheres. An alternative would be to fix the internal density of the spheres and calculate the masses based on their volumes. Our own experience suggests that this change does not have a pronounced impact on the packings generated, though we have not explored this issue in great detail. If the collisions were simply elastic, postcollision velocities for sphere systems can be calculated using simple momentum and energy balances. The growth of the spheres, however, requires that a small amount of additional energy be imparted to each sphere during each collision. This is because the growth of the spheres causes the sphere surfaces to move towards one another more rapidly than do the sphere centers. Consequently, it is necessary to force the spheres to move apart slightly more rapidly than would be predicted from an elastic collision. The additional velocity provided to a sphere is equal in magnitude to the rate of increase of that sphere’s radius and oriented along the line of the sphere centers. For monodisperse spheres, this means an equal change in the velocity of each sphere, but in opposite directions, leaving the velocity of the center-of-mass of the system unchanged (as is the case in the original L–S algorithm). For spheres of different sizes, however, this formulation imparts a larger change in velocity to the larger sphere. Thus, the center-of-mass velocity in the present version of the algorithm is not conserved during the collision. This method of allocating the additional energy is not unique and other possible allocations may work equally well. Over

time the additional energy created during collisions would accelerate the spheres, but this is avoided by regularly rescaling the velocities to hold the mean speed constant.

These changes allow the L–S algorithm to generate a dense packing of polydisperse spheres in a concurrent fashion. While the changes themselves are relatively straightforward, the resulting algorithm runs significantly more slowly than the monodisperse version. This is caused in large part by the use of neighbor lists in the algorithm. Neighbor lists are a standard method in molecular dynamics simulations to increase the efficiency of the calculation for the time at which the next collision occurs.<sup>15</sup> Essentially, these lists restrict the number of candidates with which any given sphere may collide to those that are nearest the sphere. In polydisperse systems, however, the number of candidates that must be included may be significantly larger than in monodisperse systems. This is because a single large particle may have many small particles as nearest neighbors. In addition, because large particles grow more rapidly, the neighbor lists must also be updated more frequently than in monodisperse simulations. As a result, a 10 000 sphere system with a large range of particle volumes requires roughly 48 h to run on a 1 GHz Pentium computer, while a comparably sized monodisperse system could be run in approximately 1 h. Both algorithms scale as roughly  $N^2$  in execution time, where  $N$  is the total number of spheres.

### III. RECURSIVE BINARY PACKINGS

One simple mechanism for creating a dense, amorphous packing in a binary system of spheres is to first create a packing of only the large spheres and then to fill the remaining free space with a random packing of the small spheres. Given a fixed volume fraction to which monodisperse spheres can be randomly packed,  $\phi_m$ , the most naive estimate of the packing fraction obtainable using this recursive packing method,  $\phi_0$ , is

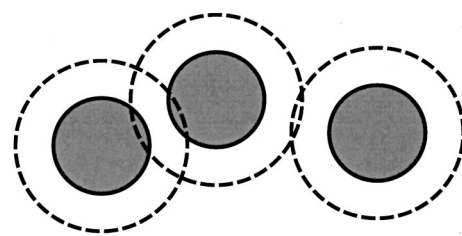
$$\phi_0 = \phi_m + (1 - \phi_m)\phi_m. \quad (2)$$

Equation (2) assumes that a full random packing of large spheres is created first (occupying  $\phi_m$ ) and then the remaining space is also packed to a volume fraction of  $\phi_m$  using the small spheres. For  $\phi_m = 0.64$ , this recursive method leads to a maximum packing fraction of  $\phi_0 = 0.87$ . Note that this approximation is similar in form to the strict bounds on the packing fraction of multiscale packings discussed by Torquato.<sup>16</sup> Specifically, if we do not constrain our consideration to random packings, then the maximum packing fraction attainable by a binary packing in three dimensions,  $\phi_{\text{strict}}$ , is bounded by

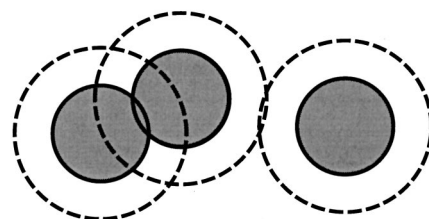
$$\phi_{\text{fcc}} \leq \phi_{\text{strict}} \leq 1 - (1 - \phi_{\text{fcc}})^2, \quad (3)$$

where  $\phi_{\text{fcc}} \approx 0.74048$  is the packing fraction of the fcc lattice (i.e., the densest possible packing of monodisperse spheres). The packing fraction of any amorphous binary system is, in turn, bounded from above by  $\phi_{\text{strict}} \approx 0.93265$ .

A simple example, however, will suffice to show that the estimate in Eq. (2) can be very inaccurate. Consider a system in which we have two types of spheres, one type of diameter  $\sigma_a$  and a second of diameter  $\sigma_b$ . Equation (2) suggests that



**Permissible Configuration**



**Impermissible Configuration**

FIG. 2. Two-dimensional schematics illustrating valid and invalid configurations in the cherrypit model. Three interpenetrable spheres are shown. The hard-cores of the spheres (shown in gray) cannot penetrate one another. The outer shells, indicated by the dashed lines, can be penetrated by one another and by the cores. In the bottom configuration, the hard cores of the two spheres on the left overlap. This is not permitted in the cherrypit model.

for any combination of  $\sigma_a$  and  $\sigma_b$ , it is possible to pack them to a packing fraction  $\phi_0 = 0.87$ . But if we let  $\sigma_a = \sigma_b$ , then we have a monodisperse packing and the maximum packing fraction is  $\phi_m = 0.64$ .

This gross overestimation of the maximum attainable packing fraction is caused, in large part, because Eq. (2) ignores the excluded volume which surrounds the first set of spheres placed. Consider a packing of large spheres of diameter  $\sigma_L$ . These spheres can be placed anywhere in space so that they will not overlap another sphere. Thus all of space can be filled to a packing fraction of  $\phi_m$ . When the next set of spheres (the small spheres of diameter  $\sigma_S$ ) is placed, however, they cannot be placed in all of the space not filled by the large spheres. Instead, they must be placed such that their centers are at least a distance  $\sigma_S/2$  away from the surface of any large sphere. Thus only a fraction of the space not occupied by the large spheres can be packed by the smaller spheres.

To get a better estimate of the volume fraction of bidisperse spheres packed recursively, we can use the interpenetrable sphere (or “cherrypit”) model.<sup>16,17</sup> In this model each sphere has a hard-core which is surrounded by a penetrable shell. A two-dimensional sketch of these spheres is shown in Fig. 2. Each interpenetrable sphere has a hard core, which cannot overlap any other sphere’s core. Surrounding these cores is an outer shell which can be penetrated by the hard cores. Letting the hard cores correspond to the large spheres in our bidisperse packing, any packing of large spheres is a permissible packing in the cherrypit model. We can then let the thickness of the shell around each large sphere correspond to the radius of the small spheres. In doing so, we see that the space occupied by the interpenetrable spheres, in-

cluding the outer shells, is the region that is inaccessible to the small sphere's centers. As such a better estimate of the packing fraction of a recursive packing of bidisperse spheres,  $\phi_{cp}$ , is

$$\phi_{cp} = \phi_m + \phi_{\text{available}} \phi_m, \quad (4)$$

where  $\phi_{\text{available}}$  is the fraction of space not filled by the large spheres or their surrounding shells. Assuming that the hard-core configurations are taken from the equilibrium ensemble in three dimensions, Torquato<sup>16</sup> showed that the fraction of space available to the small spheres is given by

$$\phi_{\text{available}}(\eta, \lambda) = (1 - \eta\lambda^3) \exp \left[ - \frac{(1 - \lambda^3)\eta}{(1 - \eta\lambda^3)^3} \right] A(\eta, \lambda), \quad (5)$$

where

$$A(\eta, \lambda) = \exp \left\{ - \frac{\eta^2 \lambda^3 (\lambda - 1)}{2(1 - \eta\lambda^3)^3} [(7\lambda^2 + 7\lambda - 2) - 2\eta\lambda^3(7\lambda^2 - 5\lambda + 1) + \eta^2 \lambda^6(5\lambda^2 - 7\lambda + 2)] \right\}.$$

In this expression,  $\eta$  is the packing fraction of the hard cores (i.e., the packing fraction of the large spheres), while  $\lambda$  is the ratio of the core diameter ( $\sigma_L$ ) to the total diameter of an interpenetrable particle ( $\sigma_L + \sigma_S$ ).<sup>16</sup> If we are interested in examining dense, random packings, the hard cores are not in equilibrium. However, monodisperse packings can be thought of as the metastable extension of the equilibrium hard sphere fluid.<sup>4</sup> As such, while Eq. (5) is not exact for our system, it is likely to be a very good approximation.

To test this result, we can create a recursive packing of bidisperse hard spheres. We begin by creating two monodisperse packings, one of large spheres and a second of small spheres, using the L-S algorithm. Both of these packings should be generated for the same size simulation box, with the number of spheres in each packing determined by the volume ratio desired, as well as some limits on the maximum and minimum number of spheres. We have required that at least 30 spheres be present in the large sphere packings and that at least 1000 spheres be present in the final combined packing. Both of the individual packings will have a packing fraction of  $\phi \approx 0.64$ . We then combine the two packings, discarding any small spheres that overlap with the large spheres. The packing fraction of such packings is plotted in Fig. 3 for several ratios of particle volumes. Also plotted in the figure is the packing fraction predicted by Eq. (4). Note that for all volume ratios, the packing fraction obtained in the simulation procedure is very close to the predicted value. One packing was generated for each volume ratio; averaging over many packings would likely increase the agreement between the simulated packings and the predicted fractions. However, the agreement shown in Fig. 3 is sufficient to conclude that Eq. (5) is a good approximation of the free space in a bidisperse packing.

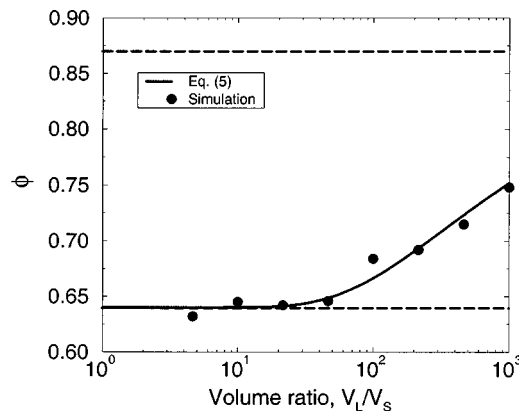


FIG. 3. A plot of the packing fraction of bidisperse sphere systems created recursively as a function of the volume ratio of the sphere. The long dashed lines indicate the assumed packing fraction of a monodisperse sphere system ( $\phi_m = 0.64$ ) and the packing fraction of a bidisperse packing calculated from Eq. (2). Note that in one case (a volume ratio of 4.64) the bidisperse packing fraction is below  $\phi_m$ . This occurs because the large sphere monodisperse packing generated in that example had a relatively low packing fraction (i.e., the estimate of  $\phi_m$  was incorrect for that particular configuration).

#### IV. LUBACHEVSKY-STILLINGER BINARY PACKINGS

From Fig. 3, it is clear that the recursive method is able to pack bidisperse spheres efficiently only in the limit of a very large volume ratio between the two types of spheres. This is because no effort is made to restrict the excluded volume in the large sphere packing. It is reasonable to conjecture that for smaller volume ratios a concurrent method could produce higher packing fractions than the recursive method by generating local particle arrangements that minimize the amount of excluded volume.<sup>18,19</sup> We have employed the extended L-S algorithm to produce amorphous (as evidenced by the radial distribution function discussed below) packings of binary sphere mixtures over a wide range of sphere volume ratios. By packing the complete mixture concurrently, it is possible to take advantage of collective arrangements of large and small spheres that will allow for higher packing fractions. An example of efficient collective packings are the (ordered) superlattices that some binary hard sphere systems can adopt with packing fractions that exceed that of the monodisperse fcc crystal.<sup>11,20</sup> While we are interested in amorphous packings, the same principle of taking advantage of collective packings with a higher local packing fraction than possible in an amorphous monodisperse system still applies.

To employ the L-S algorithm for a binary system it is necessary to choose several parameters for each packing. First, it is necessary to specify a growth rate for the spheres. Because the difference in sphere sizes tends to suppress crystallization, any reasonable growth rate should produce amorphous packings. Limited computational experimentation has shown that the final packing fraction of a bidisperse packing does not have a strong dependence on the growth rate (in contrast to monodisperse systems). For this reason, we have chosen a rapid growth rate ( $\delta = 0.1$ ) to minimize the time required for the simulation. A more important parameter is the ratio of sphere volumes. We have investigated spheres over a range of volume ratios extending from  $V_L/V_S = 1$  to

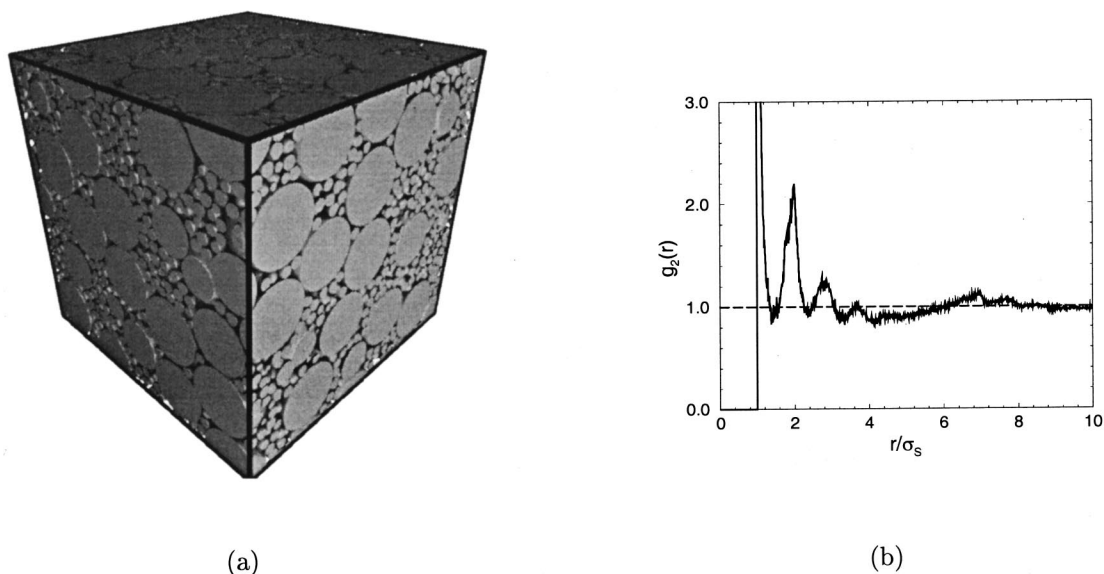


FIG. 4. (a) Sample packing resulting from the modified Lubachevsky–Stillinger algorithm applied to a binary mixture in which the volume ratio is  $V_L/V_S = 215$ . (b) The radial distribution function of the small spheres in this packing. The dashed line indicates a value of unity. Note that minima are not significantly below the dashed line compared to a dense monodisperse packing.

$V_L/V_S = 1000$ , where  $V_L$  and  $V_S$  are the volumes of the large and small spheres, respectively. In addition, we need to specify the number of large and small spheres in each packing. We have chosen to set the number of small spheres per large sphere,  $x_S$ , as

$$x_S = \frac{1}{3} \frac{V_L}{V_S}. \quad (6)$$

This number ratio fixes the total volume of the small spheres to be  $1/3$  the total volume of the large spheres. This is close to the total volume ratio that would be predicted based on Eq. (2). Defining the number of spheres in our system in this fashion does create a computational hurdle, however. In particular, at large volume ratios there are many times more small spheres than large. However, we still must include enough large spheres to generate a dense packing so the total number of spheres in the system can become quite large. We have chosen to set the minimum number of large spheres at 30 and the minimum number of total spheres at 1000. In the most extreme volume ratios considered here, this requires a system of 10 000 spheres.

Figure 4(a) shows an example of a resulting packing with a volume ratio of  $V_L/V_S = 215$ . It is difficult to appreciate any order in this system from a visual inspection of the packing. More quantitative evidence is given by the radial distribution function shown in Fig. 4(b). Before discussing the features of this plot, it is necessary to elaborate on the exact nature of the radial distribution function considered. In particular, we have only considered the presence of the smaller spheres in this calculation. One could also evaluate the radial distribution function in which only the large spheres are considered or one considering both types of spheres, but the small proportion of large spheres makes such a calculation more prone to error. As can be seen from the figure, beyond 4 small sphere diameters, the radial distribu-

tion function becomes quite flat. The presence of the large spheres can be seen in the gradual increase in the radial distribution function between 5 and 7 diameters (the large sphere diameter is approximately 6 times that of the small spheres for this volume ratio). The presence of the large spheres also introduces a substantial short-range density correlation among the small spheres as can be observed by noting that the first two minima of the radial distribution function dip only slightly below unity (as compared to a dense monodisperse sphere packing).

To avoid excessive computational costs, 100 configurations were generated for  $V_L/V_S \leq 100$  while only 10 configurations were generated for each larger volume ratio. The results of these simulations are plotted in Fig. 5. Also shown in the figure are the packing fractions of binary systems predicted or observed using several other approaches. Both Clarke and Wiley<sup>18</sup> and He *et al.*<sup>19</sup> have developed Monte Carlo methods for packing spheres based on minimizing overlaps in a system in which the sphere centers are initially uncorrelated. Yerazunis *et al.*<sup>21</sup> generated experimental packings of binary mixtures for a variety of different sphere sizes. In that work an empirical “distortion parameter” is used to model the deviation of the packing fraction from the limit of an infinite volume ratio. Also shown in Fig. 5 are the packing fractions of some dense superlattices.<sup>20</sup> The number ratios required to form such superlattices are not generally the same as the value of  $x_S$  defined by Eq. (6), but the maximum packing fractions possible for such structures still serve as a useful comparison. Finally, the density of several packings generated using the recursive method outlined in the previous section are shown as well. Again the number ratios in these systems differs from those of the concurrent packings.

As expected, the concurrent packing methods produce packings appreciably more dense than those resulting from the recursive method. It is interesting to note the striking

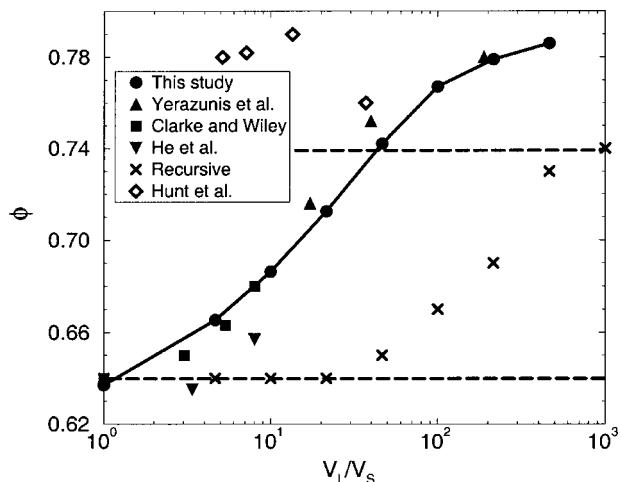


FIG. 5. Packing fraction of bidisperse sphere systems using several approaches as a function of the volume ratio between large and small spheres. The solid symbols indicate random packings generated using concurrent methods (simulation or experimental). The packing fraction predicted by Eq. (5) are indicated by "×" symbols. The open diamonds are ordered superlattice packings. The dashed lines indicate the assumed density of an amorphous monodisperse packing ( $\phi_m=0.64$ ) and the density of the pure crystal fcc lattice ( $\phi_{fcc}=0.74$ ). The solid line is drawn as a guide for the eye.

agreement in the packing fractions obtained using the extended L–S algorithm with those from the Monte Carlo methods for small volume ratios, and with those obtained experimentally at high volume ratios. While such agreement has proven to be misleading in the case of monodisperse sphere systems,<sup>7</sup> it still forms a useful starting point for the theoretical consideration of dense binary packings.

At sufficiently high volume ratios ( $V_L/V_S > 40$ ), the amorphous packings produced using the extended L–S algorithm have a higher packing fraction than the phase separated system of pure crystals. This is particularly relevant in view of the hypothesis put forth by Sanders<sup>22</sup> that a superlattice will form only if its maximum packing fraction exceeds that of the phase-separated system. The same type of space-filling agreement then suggests that the amorphous state should be more stable than a phase separated system of pure fcc crystals in the case of large volume ratio and high packing fractions. This observation is supported by the experimental evidence of Imhof and Dhont,<sup>12</sup> who found a stable glassy phase under these conditions (see Fig. 1). The comparison of packing fraction between the amorphous binary systems with the superlattices also raises interesting questions. Foremost is the question of what superlattice structure has the maximum packing fraction for large sphere volume ratios. The results presented here offer a lower bound on the maximum packing fraction that would be necessary in a superlattice to have an ordered phase develop spontaneously at high packing fractions.

In addition, as the volume ratio increases, the improvement relative to the recursive method initially becomes greater. Interestingly, however, for  $V_L/V_S > 100$  the improvement relative to the recursive packing method begins to decline. In the infinite volume ratio limit, the recursive packing method should produce the most dense amorphous packings possible ( $\phi_{cp}=0.87$ ). At intermediate volume fractions,

however, we are not aware of any strict bound that prevents the packing fraction of an amorphous bidisperse system from exceeding this limit. Whether such a high packing fraction is physically realizable is an open question.

## V. CONCLUSIONS

We have outlined the extension of the Lubachevsky–Stillinger algorithm for the concurrent generation of dense polydisperse sphere systems. By allowing each sphere to grow at a rate proportional to its initial diameter, we maintain the same distribution of sphere volumes as in a given initial condition. Because the initial condition is a very dilute configuration, a wide range of polydispersity can be easily handled using this algorithm.

Using the extended L–S algorithm, we have considered the packing of a binary sphere mixture over a wide range of sphere volume ratios. This method is effective for significantly greater volume ratios than have been previously demonstrated in the literature. As such, it allows both small and large volume ratios to be considered within a single framework. Using the interpenetrable sphere model, we can accurately approximate the maximum packing fraction that a recursive packing algorithm could obtain. We show that the L–S algorithm is able to pack bidisperse spheres significantly more efficiently than a recursive method over the range of sphere volume ratios considered here. At large volume ratios, the improvement in packing fraction using a concurrent method vs a recursive method begins to decline, perhaps because both are approaching the same limit.

Interestingly, the packing fractions presented here are consistent with those obtained by other packing algorithms. This consistency represents an attractive starting point for further theoretical investigations of binary sphere packings. For example, it is reasonable to ask if it is possible to create slightly higher packing fractions by introducing some degree of order to the system. Another challenging direction for future research is the investigation of order in binary systems. For example, one could ask if a state analogous to the maximally random jammed state defined by Torquato *et al.*<sup>7</sup> could be identified for a binary system. Finally, we note that in a future study we will apply the concurrent algorithm to investigate packing in the analogous two-dimensional problem, i.e., the packing of hard circular disks with a polydispersity in size. Here it will be interesting to determine to what degree the tendency for disk packings to crystallize persists as the degree of polydispersity increases. Another fascinating issue worth exploring is the extent to which order in binary disk packings can be controlled.<sup>23</sup>

## ACKNOWLEDGMENT

One of the authors (S.T.) was supported by the Petroleum Research Fund as administered by the American Chemical Society.

<sup>1</sup>B. D. Lubachevsky and F. H. Stillinger, *J. Stat. Phys.* **60**, 561 (1990).

<sup>2</sup>T. I. Quickenden and G. K. Tan, *J. Colloid Interface Sci.* **48**, 382 (1974).

<sup>3</sup>A. Z. Zinchenko, *J. Comput. Phys.* **114**, 298 (1994).

<sup>4</sup>M. Rintoul and S. Torquato, *Phys. Rev. Lett.* **77**, 4198 (1996).

- <sup>5</sup>S.-E. Phan, W. B. Russel, J. Zhu, and P. Chaikin, *J. Chem. Phys.* **108**, 9789 (1998).
- <sup>6</sup>W. Schaertl and H. Sillescu, *J. Stat. Phys.* **77**, 1007 (1994).
- <sup>7</sup>S. Torquato, T. M. Truskett, and P. G. Debenetti, *Phys. Rev. Lett.* **84**, 2064 (2000).
- <sup>8</sup>S. Torquato and F. H. Stillinger, *J. Phys. Chem.* **105**, 11849 (2001).
- <sup>9</sup>A. Donev, S. Torquato, F. H. Stillinger, and R. Connelly (in preparation).
- <sup>10</sup>T. Biben and J. P. Hansen, *Phys. Rev. Lett.* **66**, 2215 (1991).
- <sup>11</sup>M. D. Eldridge, P. A. Madden, and D. Frenkel, *Nature (London)* **365**, 35 (1993).
- <sup>12</sup>A. Imhof and J. K. G. Dhont, *Phys. Rev. Lett.* **75**, 1662 (1995).
- <sup>13</sup>E. Velasco, G. Navsues, and L. Mederos, *Phys. Rev. E* **60**, 3158 (1999).
- <sup>14</sup>D. W. Cooper, *Phys. Rev. A* **38**, 522 (1988).
- <sup>15</sup>M. Allen and D. Tildesley, *Computer Simulation of Liquids* (Clarendon, Oxford, 1984).
- <sup>16</sup>S. Torquato, *Random Heterogeneous Materials: Microstructure and Macroscopic Properties* (Springer, New York, 2002).
- <sup>17</sup>S. Torquato, *J. Chem. Phys.* **81**, 5079 (1984).
- <sup>18</sup>A. S. Clarke and J. D. Wiley, *Phys. Rev. B* **35**, 7350 (1987).
- <sup>19</sup>D. He, N. N. Ekere, and L. Cai, *Phys. Rev. E* **60**, 7098 (1999).
- <sup>20</sup>N. Hunt, R. Jardine, and P. Bartlett, *Phys. Rev. E* **62**, 900 (2000).
- <sup>21</sup>S. Yerazunis, S. W. Cornell, and B. Winter, *Nature (London)* **207**, 835 (1965).
- <sup>22</sup>J. V. Sanders, *Philos. Mag. A* **42**, 721 (1980).
- <sup>23</sup>A. R. Kansal, T. M. Truskett, and S. Torquato, *J. Chem. Phys.* **113**, 4844 (2000).